Boundary element simulation of bone tissue

Vannessa Duarte*, Yomar González and Miguel Cerrolaza

Instituto Nacional de Bioingeniería,
Universidad Central de Venezuela,
Ciudad Universitaria, Caracas, Venezuela
E-mail: vannessa.duarte@inabio.edu.ve
E-mail: yomar.gonzalez@inabio.edu.ve
E-mail: miguel.cerrolaza@inabio.edu.ve
*Corresponding author

Abstract: Usually the mechanical condition and the induced electric signal are devoted to be part of the stimuli controlling the biophysical activity associate with healing and remodelling phenomena. The tissue differentiation theory proposed by Claes and Heigele (1999) has been numerically implemented using an poroelastic boundary element framework to characterises fracture healing, leading to a new poroelastic correlation between mechanical conditions and local tissue formation. This paper also presents the implementation of the piezoelectric boundary integral equation to further study the bone tissue behaviour. The results were in good agreement with those reported in previous works.

Keywords: boundary element method; bone healing; tissue differentiation; piezoelectricity; poroelasticity; radon transform; axisymmetry; anisotropy.

Reference to this paper should be made as follows: Duarte, V., González, Y. and Cerrolaza, M. (2011) 'Boundary element simulation of bone tissue', *Int. J. Biomedical Engineering and Technology*, Vol. 5, Nos. 2/3, pp.211–228.

Biographical notes: Vannessa Duarte is an Engineer in Computer Science (2005), graduated from the Universidad Nacional Experimental del Táchira, Venezuela. Currently she is working to complete her Doctor in Engineering Science Degree from the Universidad Central de Venezuela. Her research interest includes numerical methods and piezoelectric behaviour of bone. She also has worked in various research topics including medical signal processing.

Yomar González is a Mechanical Engineer (2001), graduated from the Universidad Central de Venezuela. He received the Doctor in Engineering Science Degree from the Universidad Central de Venezuela (2007). He is currently teaching numerical methods at the postgraduate program of Structural Engineering and Bioengineering. He is also the Research Coordinator of the Instituto Nacional de Bioingeniería. His research is oriented towards mechanical simulation of the bone healing process and bone remodelling. Other research interest includes design of biomedical devices.

Miguel Cerrolaza is a Civil Engineer from the Universidad Central de Venezuela (1980), Master of Sciences from the Federal University of Rio de Janeiro (Brazil, 1981), Dr.Eng. from the Universidad Politécnica de Madrid (Spain, 1988) and PostDoc from the Ecole Nationale des Ponts et Chaussees (Paris, France, 1995). Currently, he is a full Professor of the Universidad Central de Venezuela. Since 1997, he is the head of the Instituto Nacional de Bioingeniería. His main interests are biomechanics and biofluids, finite and boundary element methods in engineering and genetic algorithms in engineering optimisation.

1 Introduction

The computational mechanobiology has been widely used to describe the changes in cell expression, the composition, structure and phenotype of bone tissues, as a function of the applied mechanical stimuli. However, in the last decade, other factors have also been incorporate to formulate a more generalised bone response hypotheses, like locally expressed growth factors (Bailón-Plaza and Van der Meulen, 2001), cell-to-cell interactions (Stains and Civitelli, 2005), drugs release (Hernández et al., 2001; Zeman and Cerrolaza, 2005), osteoinductive bone morphogenetic proteins (Blokhuis et al., 2001) and the piezoelectric effect (Schmidt-Rohlfinga et al., 2002; Ramtani, 2008) among other.

Regardless of the case, the simulation of bone repair and remodelling is also dependent of the applied numerical method capabilities (Finite Element Method, FEM; Finite Difference Method, FDM; etc.). Recently, the Boundary Element Method (BEM) has shown to be an effective alternative to the more familiar FEM and FDM to predict the effect on biomechanical response of bone (Martínez et al., 2006; González et al., 2009). The boundary scheme brings some advantages to simulate the callus formation during bone healing. In that case, moving outward surfaces, ossification paths and the calculation of the properties evolution are usually defined as a function of only-boundary values, where the governing differential equations are satisfied exactly.

1.1 Bone healing

Once a fracture occurs, a very complex process is auto-activated naturally to repair the injury. Fracture healing involves the generation of intermediate tissues, such as fibrous connective tissue, cartilage and woven bone, with different paths being governed by a variety of stimulating agents like the mechanical environment, hormonal and physiological patterns, geometric configuration of the fracture fragments and growth factors (Lacroix et al., 2002).

We can differentiate between primary or secondary fracture healing. However, in most cases, which involve moderate gap sizes and fracture stability, heals by secondary fracture healing forming a voluminous callus. This type of healing benefits from a certain amount of inter-fragmentary movement at the fracture site and has a series of sequential stages than can overlap to a certain extent, including inflammation, callus differentiation, ossification and remodelling. Bone ossification

can occur mainly by endochondral and intramembranous ossification. In the first, cartilage is formed, calcified and replaced by bone. In the second, bone is formed directly by osteoblasts. As depicted in Figure 1, the process involves the coordinated participation of migration, differentiation and proliferation of inflammatory cells, angioblasts, fibroblasts, chondroblasts and osteoblasts.

Figure 1 The mesengenic process

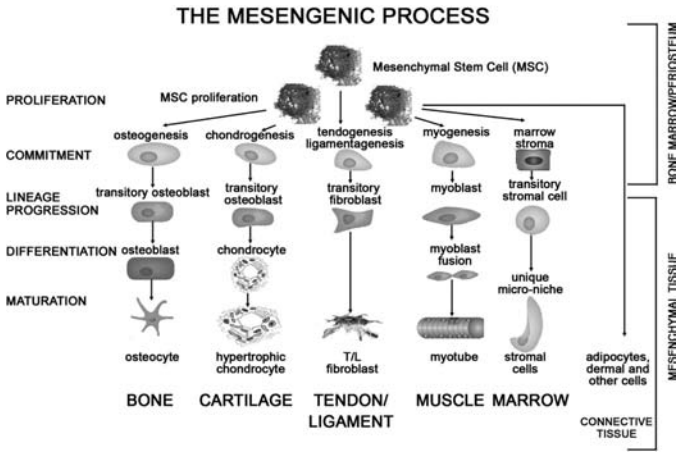

Source: Caplan and Boyan (1994)

Healing begins as undifferentiated mesenchymal cells migrating from the surrounding soft tissue to produce initial connective tissue around the fracture site.

Next stages, involve cartilage and bone tissue formation (Figure 2). Once the callus is filled (mainly by cartilage), endochondral ossification begins following a complex sequence of cellular events including cartilage maturation and degradation, vascularity and osteogenesis (Figure 3). The ossification continues until all the cartilage has been replaced by bone with sufficient stiffness. Last, remodelling of the fracture site begins gradually in order to restore the original internal structure and shape (Doblaré et al., 2004)

1.2 Boundary element approaches in bone modelling

Attempts have been made to use the BEM in the simulation of biological problems. A few interesting works have been published illustrating the versatility of the method in this area. The external bone remodelling model proposed by Martínez et al. (2006) assumed that level of damage and the strain energy near the periosteum and endosteum completely controls the process. BEM was used to evaluate the displacements and tractions field and modify the geometry according to remodelling law. Later, Annicchiarico et al. (2007) implemented smoothing techniques like β-spline, to integrate the geometry in the boundary integral equation used to simulate the external bone remodelling phenomena following the model proposed by Martínez et al. (2006). Sfantos and Aliabadi (2007) proposed an alternative boundary element formulation to simulate three-dimensional wear in artificial hip joints. A parametric study of the wear evolution was carried out, including

different update periods for the worn geometry of the acetabular cup, different loading angles, different femoral head sizes and different materials combinations, all under the same variable loading conditions based on the hip activity. Other works include the application of BEM and genetic algorithms for cavity detection in cortical bone, using a point load superposition technique (Ojeda et al., 2007, 2008). Gámez et al. (2007) presented an effective artificial sub-sectioning technique with a region-by-region iterative algorithm for parallel computation for detection of cracks in diaphysis sections of cortical bone.

Figure 2 Fracture healing process (http://www.bonestimulation.com)

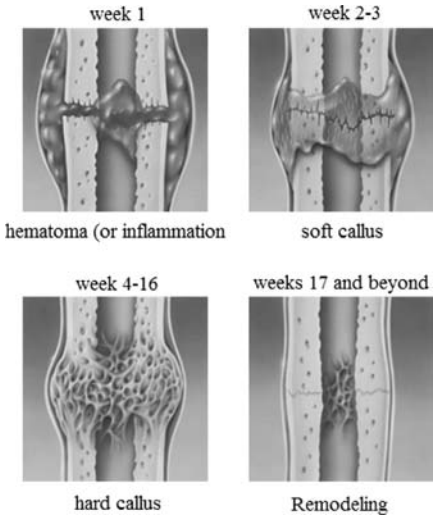

Figure 3 Callus phenotype at day 9 after fracture. Notice the intramembranous ossification process close to the periosteum and the chondrogenesis present in most of fracture site (http://www.uwo.ca)

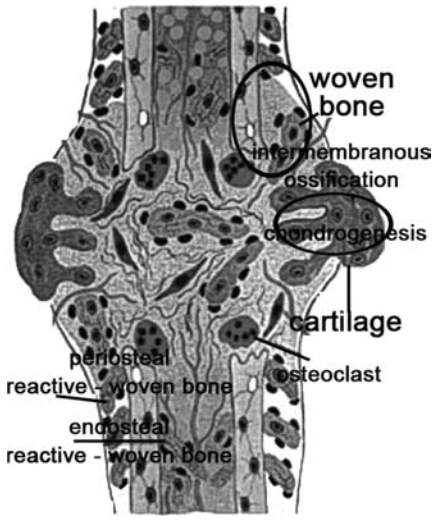

2 Materials and methods

Bone is usually considered as a composite material with interconnected pores in the elastic solid matrix (Papathanasopoulou et al., 2002; Lacroix and Prendergast, 2002; Gómez et al., 2005; Isaksson et al., 2006; García et al., 2007). The recent multiphasic porous models involved the solid osseous matrix, the extracellular fluid phase, the osteoblastic cellular phase, the fluid velocity and the pore pressure promoting the cellular activity. The bone matrix also exhibits piezoelectric properties strongly associated with the fluid transport effect and the independent mass and charge densities between the fluid and solid component (Ramtani, 2008). These parameters help to further predict the constitutive response of bone even at cellular level. The following attempts are mainly concerned with the development of suitable BEM algorithms to study the bone behaviour from a poroelastic and piezoelectric point of view.

2.1 Boundary element method for poroelastic media

The poroelastic code presented is part of BEM codes to establish a callus growth model. It contains the axisymmetric fundamental solutions for steady-state poroelastic problems in a linear-elastic, isotropic and non-homogeneous media, following the Biot consolidation theory (Biot, 1956). The constitutive equations for three-dimensional consolidation, written in the cartesian form are

$$(\lambda+\mu)u_{j,ij}+\mu u_{i,jj}-\beta p_{,i}+f_i=0 \tag{1}$$

$$kp_{,jj}-\left(\frac{\beta^2}{\lambda_u-\lambda}\right)\dot{p}-\beta\dot{u}_{j,j}+\psi=0 \tag{2}$$

where u_i represents the displacement, p is the excess pore pressure, f_i is the body force per unit volumen and ψ is the time rate of volumetric fluid supply per unit volumen.

Meanwhile, λ and μ are the drained Lamb-elastic constants, λ_u is the undrained elastic modulus, k is the permeability and β is a function of B, called the compressibility coefficient or Skempton pore pressure coefficient. The uncoupled poroelastic boundary integral equation for axi-symmetric bodies, follows the matrix form (3). The generalised quasi-static displacements and tractions are transformed into a cylindrical coordinate system (r,ϕ,z) and then circuferential integration is carried out (Balas et al., 1989; Dargush and Banerjee, 1991, 1992).

$$\begin{aligned}
&\begin{bmatrix} C_{rr}(P)\,C_{rz}(P)\,C_{r\theta}(P)\\ C_{zr}(P)\,C_{zz}(P)\,C_{z\theta}(P)\\ C_{\theta r}(P)\,C_{\theta z}(P)\,C_{\theta\theta}(P)\end{bmatrix}\begin{bmatrix} U_r(P)\\ U_z(P)\\ \theta(P)\end{bmatrix}\\
&=2\pi\int_\Gamma\begin{bmatrix} U^*_{rr}(P,Q)\,U^*_{rz}(P,Q)\,U^*_{r\theta}(P,Q)\\ U^*_{zr}(P,Q)\,U^*_{zz}(P,Q)\,U^*_{z\theta}(P,Q)\\ U^*_{\theta r}(P,Q)\,U^*_{\theta z}(P,Q)\,U^*_{\theta\theta}(P,Q)\end{bmatrix}\begin{bmatrix} T_r(Q)\\ T_z(Q)\\ q(Q)\end{bmatrix}r(Q)d\Gamma\\
&\quad-2\pi\int_\Gamma\begin{bmatrix} T^*_{rr}(P,Q)\,T^*_{rz}(P,Q)\,T^*_{r\theta}(P,Q)\\ T^*_{zr}(P,Q)\,T^*_{zz}(P,Q)\,T^*_{z\theta}(P,Q)\\ T^*_{\theta r}(P,Q)\,T^*_{\theta z}(P,Q)\,T^*_{\theta\theta}(P,Q)\end{bmatrix}\begin{bmatrix} U_r(Q)\\ U_z(Q)\\ \theta(Q)\end{bmatrix}r(Q)d\Gamma
\end{aligned} \tag{3}$$

P is the field point, Q is the integration point, $C_{\alpha\eta}(P)$ is the free term, $r(Q)$ is the radial coordinate of Q, U_r and U_z are the displacements in radial and axial direction respectively, θ is now called the excess pore pressure, T_r and T_z are the tractions in radial and axial direction respectively. $U^*_{rr}(P,Q)$, $U^*_{rz}(P,Q)$, $U^*_{zr}(P,Q)$, $U^*_{zz}(P,Q)$, $T^*_{rr}(P,Q)$, $T^*_{rz}(P,Q)$, $T^*_{zr}(P,Q)$ and $T^*_{zz}(P,Q)$ are the kernel fuctions identical to those of axi-symmetric elastic displacements and tractions (Bakr and Fenner, 1983; Balas et al., 1989). Meanwhile $U^*_{\theta\theta}(P,Q)$ and $T^*_{\theta\theta}(P,Q)$ are the potential flow axi-symmetric kernels (Bakr and Fenner, 1983; Dargush and Banerjee, 1991). $U^*_{r\theta}(P,Q)$, $U^*_{z\theta}(P,Q)$, $T^*_{r\theta}(P,Q)$ and $T^*_{z\theta}(P,Q)$ are the coupling terms (Dargush and Banerjee, 1991, 1992). The remaining components are zero due to the uncoupled theory considered.

The analytical kernels shown in equation (3) were taken from BEM quasi-static and axi-symmetric thermoelastic and poroelastic approach (Bakr and Fenner, 1983; Dargush and Banerjee, 1991; Brebbia and Domínguez, 2003; Dargush and Banerjee, 1992), as well as the asymptotic behaviour (Graciani et al., 2005).

2.2 BEM simulation of bony poroelastic media

Claes and Heigele (1999) developed a quantitative tissue differentiation theory where strain and hydrostatic pressure fields along existing calcified pathways (Figure 4(A)) determine the local tissue formation in a fracture gap. The study compares the axisymmetric FE strains/stresses with histological findings to describe progressive stiffening of the callus. A correlation between mechanical conditions and phenotypes of five tissues types with differents elastic properties tissues in a fracture callus was presented leading to a better understanding of when intramembranous or endochondral ossification would occur (Figure 4(B)). The course of interfragmentary movement (IFM) vs. healing time was also correlated.

This remarkable contribution was used as a reference to support the methodology applied to obtain new results.

Starting from a 3D lineal-elastic BEM code (Beer, 2001), the pore pressure was included into a stationary-poroelastic callus model, as a part of the stimuli function to characterise the tissue phenotype and properties in callus site. These boundary element (BEM) analysis allowed us to extend the observations made by other authors and a new poroelastic correlation is proposed. In addition to earlier quantitative theories, recent poroelastic models will be able to compare the tissue properties evolution completely, such as the elastic moduli (E) and Poisson ratio (ν), depending on both strain and pore pressure fields.

It is now clear that other factors influence the bone healing pattern, but the underlying hypothesis in this work is that a combination of local strain and pore pressure are the only stimuli to be considered.

The success of BEM algorithms was previosly established by showing that it can correctly predict the response of well known analytical solutions for problems in elasticity, thermoelasticity and poroelasticity as well (González et al., 2008, 2009). Once the method proposed was tested, the uncoupled Biot linear consolidation theory (Biot, 1956; Dargush and Banerjee, 1991) was implemented to simulate the tissue differentiation process.

Three different healing stages as depicted in Figure 5, with 3 mm of ostetomy gap and 1.2 mm of initial interfragmentary movement (IFM) were considered for the poroelastic BEM simulation, following the work done by Claes and Heigele (1999).

Material properties as shown in Table 1 (details are shown in González et al., 2009).

Figure 4 (A) Axi-symmetric simulation of the three healing stages considered and the ossification paths: (a) 1 week p.o.; (b) 4 weeks p.o.; (c) 8 weeks p.o. and (d)FEM model and boundary conditions. (OI)surface of intramembranous ossification, (OE)surface of endochondral ossification and (B) mechanical correlations proposed by Claes and Heigele (1999)

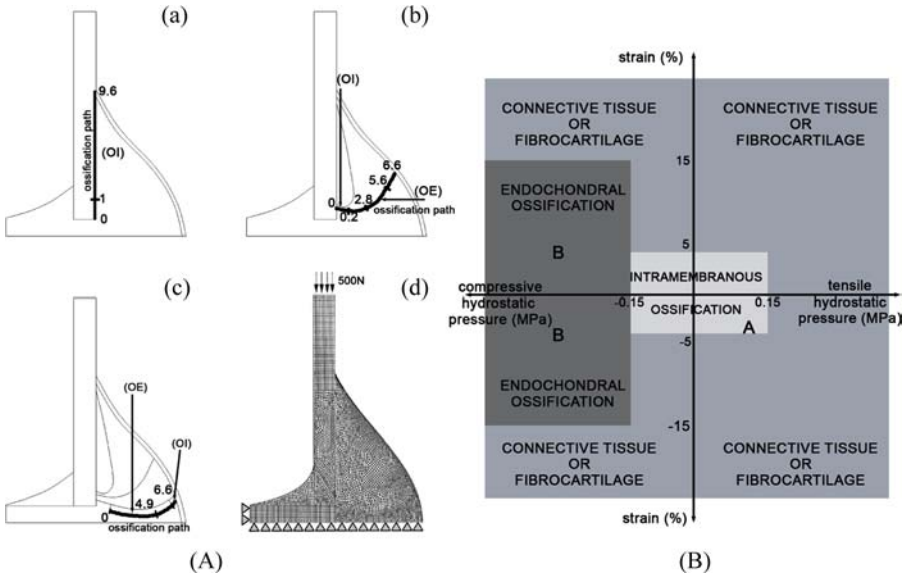

Figure 5 Axisymmetric bifasic boundary conditions at three healing stages: (a) 1 week; (b) 4 weeks and (c) 8 weeks

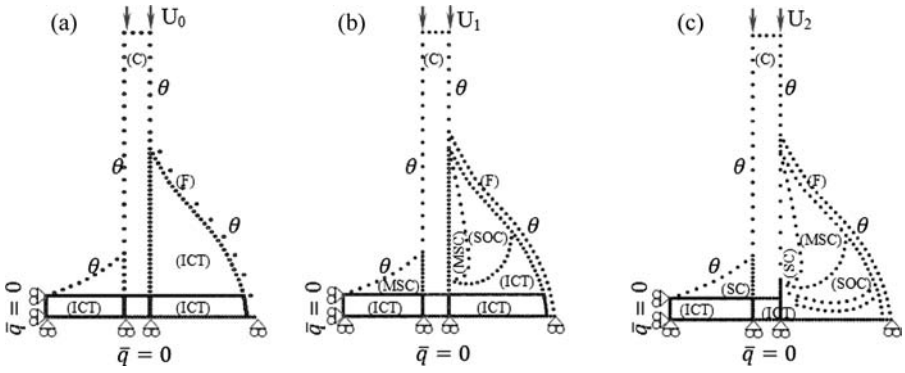

Table 1 Poroelastic properties: E (Youngs modulus), ν (drained Poissons ratio), K_s (drained modulus), K_f (undrained modulus), ϕ (porosity), k (hydraulic permeability; $k = \kappa\mu$), ν_u (undrained Poissons ratio), B (Skemptons modulus). (a) Claes and Heigele (1999); (b) Isaksson et al. (2006); (c) calculated using constitutive law

Tissue type	$E(a)$ (MPa)	$\nu^{(a)}$	$K_s^{(b)}$ (MPa)	$K_f^{(b)}$ (MPa)	$\phi(b)$	$k^{(b)}$ (m^4/Ns)	$\nu_u^{(c)}$	$B^{(c)}$
Initial connective tissue (ICT)	3	0.4	2300	2300	0.8	1.0×10^{-14}	0.5	0.998
Soft callus (SOC)	1000	0.3	3400	2300	0.8	5.0×10^{-15}	0.428	0.889
Intermediate stiffness callus (MSC)	3000	0.3	17660	2300	0.8	1.0×10^{-13}	0.384	0.53
Stiff callus (SC)	6000	0.3	17660	2300	0.8	3.7×10^{-13}	0.341	0.321
Chondroid ossification zone (COZ)	10000	0.3	13920	2300	0.8	3.7×10^{-13}	0.316	0.177
Cortex (C)	20000	0.3	17660	2300	0.04	1.0×10^{-17}	0.302	0.182
Fascie (F)	250	0.4	2300	2300	0.8	1.0×10^{-14}	0.482	0.949

On the other hand, it has been suggested by several authors (Fukada and Yasuda, 1957; Basset and Becker, 1962; Ramtani, 2008) that the piezoelectric properties of bone play an important role in the development and growth remodelling of the skeleton. According to this theory, applied stresses generate local potential gradients along the collagen fibre which provide a local stimulus for bone-generating cells (Basset and Becker, 1962; Becker et al., 1964; Ahn and Grodzinskyc, 2009). Relying on the piezoelectric properties of natural bone and their influence on the hastening of bone healing, the objective of the next application is to simulate the electro-mechanical coupled behaviour of bone tissue to a new imposed electrical field.

2.3 Boundary element method for piezoelectric media

The use of electrical stimulation as adjunctive therapy for injured bones dates back to the 1700s (Fleischli and Lauglin, 1997). Electrical properties of bone are relevant not only as an hypothesised feedback mechanism for bone adaptation and remodelling, but also in the context of external electrical stimulation of bone in order to aid its healing and repairing (Ramtani, 2008).

2.3.1 Constitutive equation

The constitutive equations of linear piezoelectricity are given by

$$C_{ijkl}u_{k,li} + e_{lij}\varphi_{,il} = 0 \tag{4}$$

$$e_{ikl}u_{k,li} - \epsilon_{il}\varphi_{,li} = 0 \tag{5}$$

in which C_{ijkl}, e_{ijk} and ϵ_{ik} are the elastic stiffness tensor, the piezoelectric tensor and the dielectric permittivity tensor respectively. u_i and $\varphi_{,k}$ are the displacements and electric potential.

On the boundary Γ of a three dimensional piezoelectric body, the displacement vector U and traction vector T are related by the boundary integral equation (6)

$$\begin{aligned}
&\begin{bmatrix} C_{xx}(P)\, C_{xy}(P)\, C_{xz}(P)\, C_{x\phi}(P) \\ C_{yx}(P)\, C_{yy}(P)\, C_{yz}(P)\, C_{y\phi}(P) \\ C_{zx}(P)\, C_{zy}(P)\, C_{zz}(P)\, C_{z\phi}(P) \\ C_{\phi x}(P)\, C_{\phi y}(P)\, C_{\phi z}(P)\, C_{\phi\phi}(P) \end{bmatrix} \begin{bmatrix} U_x(P) \\ U_y(P) \\ U_z(P) \\ \phi(P) \end{bmatrix} \\
&= \int_\Gamma \begin{bmatrix} U^*_{xx}(P,Q)\, U^*_{xy}(P,Q)\, U^*_{xz}(P,Q)\, U^*_{x\phi}(P,Q) \\ U^*_{yx}(P,Q)\, U^*_{yy}(P,Q)\, U^*_{yz}(P,Q)\, U^*_{y\phi}(P,Q) \\ U^*_{zx}(P,Q)\, U^*_{zy}(P,Q)\, U^*_{zz}(P,Q)\, U^*_{z\phi}(P,Q) \\ U^*_{\phi x}(P,Q)\, U^*_{\phi y}(P,Q)\, U^*_{\phi z}(P,Q)\, U^*_{\phi\phi}(P,Q) \end{bmatrix} \begin{bmatrix} T_x(Q) \\ T_y(Q) \\ T_z(Q) \\ q(Q) \end{bmatrix} d\Gamma \\
&- \int_\Gamma \begin{bmatrix} T^*_{xx}(P,Q)\, T^*_{xy}(P,Q)\, T^*_{xz}(P,Q)\, T^*_{x\phi}(P,Q) \\ T^*_{yx}(P,Q)\, T^*_{yy}(P,Q)\, T^*_{yz}(P,Q)\, T^*_{y\phi}(P,Q) \\ T^*_{zx}(P,Q)\, T^*_{zy}(P,Q)\, T^*_{zz}(P,Q)\, T^*_{z\phi}(P,Q) \\ T^*_{\phi x}(P,Q)\, T^*_{\phi y}(P,Q)\, T^*_{\phi z}(P,Q)\, T^*_{\phi\phi}(P,Q) \end{bmatrix} \begin{bmatrix} U_x(Q) \\ U_y(Q) \\ U_z(Q) \\ \phi(Q) \end{bmatrix} d\Gamma
\end{aligned} \tag{6}$$

2.3.2 Anisotropic piezoelectric materials

A characteristic of piezoelectric materials is its anisotropic behaviour, therefore the matrix C is an anisotropic constitutive matrix. In case of bones, the piezoelectricity appears only when the shearing force acts on the orientated collagen fibres so that they slip past one another (Silva et al., 2001) and the matrix linking the stresses and the electric field (piezoelectric matrix) is

$$\mathbf{e} = \begin{bmatrix} 0 & 0 & 0 & e_{123} & e_{113} & 0 \\ 0 & 0 & 0 & e_{113} & -e_{123} & 0 \\ e_{311} & e_{311} & e_{333} & 0 & 0 & 0 \end{bmatrix}. \tag{7}$$

The matrix relating electric displacement to the field vector tensor ϵ_{ij} is perpendicular and parallel to the longitudinal-axis and is given by

$$\epsilon = \begin{bmatrix} \epsilon_{11} & 0 & 0 \\ 0 & \epsilon_{11} & 0 \\ 0 & 0 & \epsilon_{33} \end{bmatrix}. \tag{8}$$

The fundamental solution of the differential equation for unit values of load and electric field can be derived using a Radon transformation (Thoeni, 2005; Gaul et al., 2003). The fundamental solution in 3D for U^*_{MK} which combines the displacements and the electric potential is given by

$$U^*_{MK}(r, \theta_1, \theta_2) = \frac{1}{r} G^u_{MK}(\theta_1, \theta_2), \tag{9}$$

r is the distance between P and Q (length of vector r) and θ_1, θ_2 are determined according to Figure 6, where r_0 a unit vector in the direction r (Beer et al., 2008). Because of the complexity of the fundamental solution, a scheme is adopted to estimate and storage values of G as a function of θ_1,θ_2.

2.4 BEM simulation in a bony piezoelectric media

The corresponding anisotropic 3D fundamental solution were implement into a general lineal-elastic BEM code (Beer, 2001) by changing and adding subroutines (more details in Beer et al., 2008). The code was validated with the resulting displacement solution given analytically by a normalised cube with the material constants (Table 2) presented in Denda and Wang (2009).

Table 2 Approximate values of the femur material constants[a]

e_{123}	e_{113}	e_{311}	e_{333}	C_{11}	C_{12}	C_{13}	C_{33}	C_{44}	ϵ_{11}	ϵ_{33}
177.66	55.53	15.06	18.6	21.2	9.5	10.2	37.6	7.5	10	12

[a]e_{ij} are the piezoelectric coefficients in $C/m^2 \times 10^{-5}$, C_{ij} are the elastic constants in the transversely isotropic case in GPa, ϵ_{ij} are the dielectric coefficients in $C/Vm \times 10^{-12}$.

Source: El-Naggar et al. (2001)

Bone apposition occurs in somewhat large amounts in response to a balanced alternating pulsed current (Marino and Becker, 1970). The exact mechanism

Figure 6 Calculation of angles θ_1,θ_2

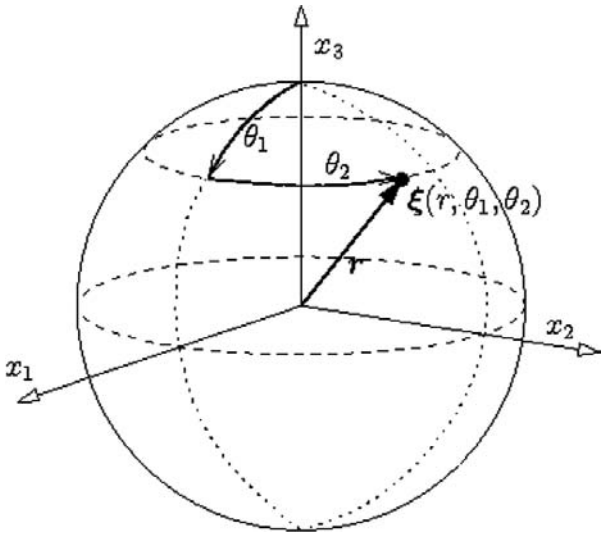

Source: Thoeni (2005)

by which the potential stimulates the growth respond is unknown. However, Gjelsvik (1973) presented a model based on four postulates: the signal for surface remodelling is the piezoelectric polarisation vector normal to the surface, material symmetry direction of new bone deposited follows the direction of the bone on which it is growing, new surface bone is deposited so that no residual stresses result and material symmetry direction tries to keep aligned with the time average of the principal stress directions in the bone. This theory proposed by Gjelsvik (1973) is using as a reference to support the methodology applied to obtain results by using Boundary Element Method.

3 Preliminary results

3.1 Poroelastic BEM

3.1.1 Inter-fragmentary motion

Even if the bone fragments are stabilised, moderate axial movement in the range of 0.2–1.0 mm in gap sizes of 3 mm are believed to promote optimal healing in transverse osteotomies (Duda et al., 1998; Claes et al., 1998). For each model (Figure 5) both the Inter-Fragmentary Displacement (IFM) and Inter-Fragmentary Strain (IFS) were calculated (see Figure 7).

The inter-fragmentary movement is sensitive to the constitutive law and did not reproduce the in vivo measurements (see Figure 7(a)). However the findings were according to the range (0.2–1.0mm) proposed to be optimal for fracture healing. Lacroix and Prendergast (2002) also studied the inter-fragmentary movement as a function of boundary conditions and time healing. They showed similar values of IFM. The differences are mostly due to the material properties used.

3.1.2 Pore pressure along the ossification path

This section shows the calculated pore pressures (Ph) along the ossification paths (see Figure 8). The origin was taken close to the periosteal surface as depicted in Figure 4(A). The results are presented illustrating the type of ossification (OI/OE) for each stage considered.

Figure 7 (a) Comparison of IFMs calculated through in vivo, FEM and BEM analyses and (b) Comparison of IFSs calculated through FEM and BEM analyses

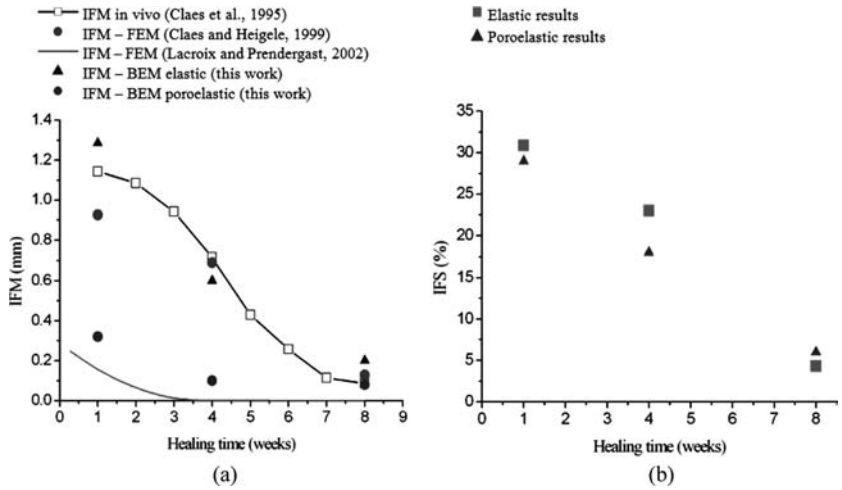

In Figure 8 the increasing of tissue stiffness is reproduced. The pore pressures were high at the beginning where a progressive volume expansion associated with the migration and differentiation of the osteoprogenitor cells is taking place. These values become moderate through healing time.

Due to the initial instability of bone fragments, the pore pressure field suggested appropriate conditions to promote ossification around the periosteum and in the major part of the endosteum area. The high strain values also corroborate this observation (details can be found in González et al., 2008, 2009). The cortical gap exhibits high pressures under compression, stimulating bone formation by endochondral process. These values become moderated toward the periosteal gap, where granulation tissue is mostly found. In the beginning of fourth week, the pressures along the new ossification path behave differently compared with the hydrostatic pressures reported by Claes and Heigele (1999). Notice the increment pressure values as we get closer to the periphereal callus area (see Figure 8). At this point, a matrix formed by cartilage is mainly seen due to endochondral ossification progress (Lacroix et al., 2002). However, the magnitudes of strains (absolute value) were small enough to stimulate the formation of cartilaginous tissue. Later, the cell differentiation process continues toward osteoclasts mostly and a new volume expansion proceeds. As the endochondral and intramembranous ossification paths find each other (Figure 5: stage b and c) and new tissues are formed, the strains become lower and the pore pressure field tends to equilibrium progressively (Figure 8).

Figure 8 Stress poroelastic results along bony surfaces using boundary element method. (OI) surface of intramembranous ossification, (OE) surface of endochondral ossification

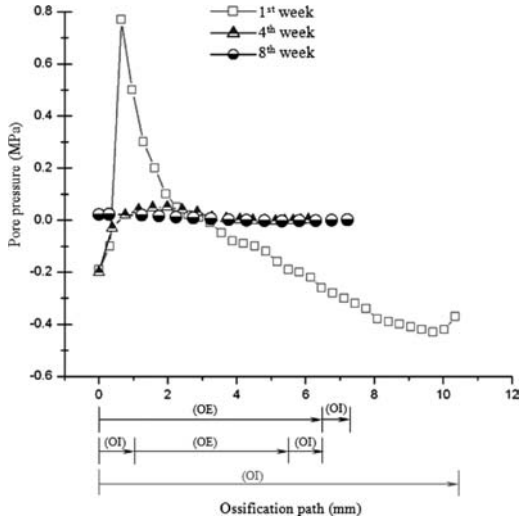

3.1.3 Proposed poroelastic correlation

Based on poroelastic-only constitutive law, a new correlation is proposed (Figure 9) and a direct quantitative comparison of the mechanical environment is now possible allowing a better understanding of the results reported by previous FEM simulations. The basic procedure was to evaluate mainly the postprocessing BEM data along the ossification paths for each stage considered, and to observe how those magnitudes defined new ranges for each tissue type according with the assumed hypothesis. The adjacent areas were also studied.

3.2 Piezoelectric BEM

3.2.1 BEM modelling of bone test specimen

In order to validate the computer code, we have considered a unit cubic bone specimen (Figure 10) loaded ($t_3 = \sigma_3 = 1$ and $t_4 = D_3 = 1$ at z = 1) at one end and fixed at the load-reacting end ($u_I = 0, I = 1, 2, 3, 4$ at z = 0). A similar example was shown by Denda and Wang (2009). According to Wolff's law, bone is deposited and reinforced at areas of large stress, which is correlated with results reported by bone growth and healing simulations. The role of the collagen piezoelectricity also influence the bone response producing the strain-generated potentials (Ahn and Grodzinskyc, 2009). The example below seems to confirm the hypothesis when the applied surface charge helps to promote areas where bone could be generated. The results help to speculate how healing process could be slightly improved with the application of charge (Figure 11). Qualitative, growth areas could be expected in the top due to the negative potential distribution (Figure 12). These results agree with Basset and Becker, 1962).

Figure 9 New correlation between poroelastic mechanical conditions and tissue types. Cartilaginous tissue was incorporated according to the Lacroix and Prendergast's findings

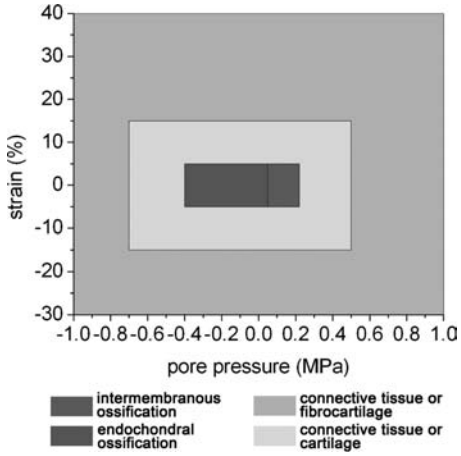

Figure 10 Discretised mesh of the cube with loading on the top ($t_3 = \sigma_3 = 1$ and $t_4 = D_3 = 1$ at z = 1) and fixed at the bottom ($u_I = 0, I = 1, 2, 3, 4$ at z = 0)

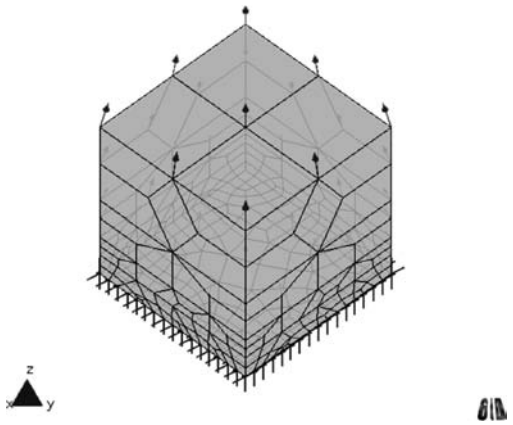

Figure 11 Displacement in the direction of the bone symmetry: (a) without charge and (b) charge on the top

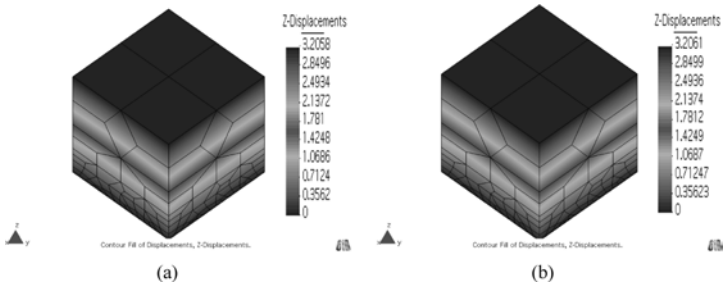

(a) (b)

Figure 12 Electric potential distribution: (a) without charge and (b) charge on the top

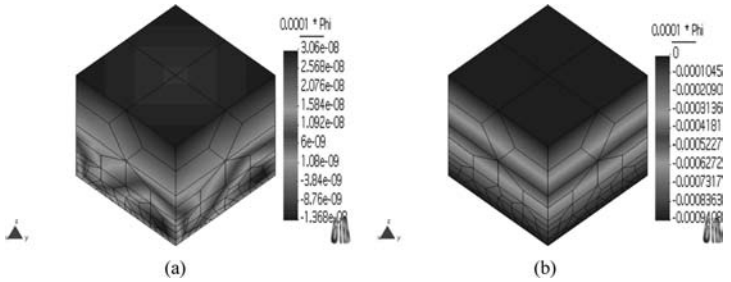

(a) (b)

4 Conclusion

This work represents an important contribution in the application of Boundary Element Method for biological problems. In particular, the capability for bone healing axi-symmetric simulation in a poroelastic media to speculate the mechanical environment during tissue differentiation process has been demonstrated.

Using a boundary framework we have characterised the phenotype tissues involved into bone healing. The poroelastic study allowed to extend the observations made by Claes and Heigele (1999) and a new poroelastic-only correlation is proposed. Although the first results are promising, it is necessary to evaluate this correlation with other experimental results.

The need to include transitory kernels into the boundary integral formulation, as well as the cell diffusion analysis and moving boundary techniques is a key aspect for future dynamic applications.

The exact mechanism by which the potential stimulates the growth respond is unknown and experimental data remains poorly understood. However, the literature available suggests that the induced potential through the bone could be an efficient alternative to improve fractures repair. The preliminary results depicted in Figures 11 and 12 are promising since areas for bone deposition arise from the imposed surface of charge. This could be a simple and qualitative validation for the electromechanical behaviour of the bone.

Acknowledgements

Support by Académia de Ciencias Físicas, Matématicas y Naturales de Venezuela, Fondo Nacional de Ciencia, Tecnología e Innovación (FONACIT) and Consejo de Desarrollo Cientifíco y Humanistico (CDCH), UCV, is gratefully acknowledged.

References

Ahn, A.C. and Grodzinskyc, A.J. (2009) 'Relevance of collagen piezoelectricity to Wolff's Law: a critical review', *Medical Engineering & Physics*, Vol. 31, No. 7, pp.733–741.

Annicchiarico, W., Martinez, G. and Cerrolaza, M. (2007) 'Boundary elements and b-spline surface modeling for medical applications', *Applied Mathematical Modelling*, Vol. 31, pp.194–208.

Bailón-Plaza, A. and Van der Meulen, M.C.H. (2001) 'A mathematical framework to study the effects of growth factor influences on fracture healing', *J. Theor. Biol.*, Vol. 212, pp.191–209.

Bakr, A.A. and Fenner, R.T. (1983) 'Boundary integral equation analysis of axisymmetric thermoelastic problems', *Journal of Strain Analysis*, Vol. 18, No. 4, pp.239–251.

Balas, J., Slâdek, J. and Slâdek, V. (1989) *Stress Analysis by Boundary Element Method*, Elsevier, Amsterdam.

Basset, C.A.L. and Becker, R.O. (1962) 'Generation of electric potential by bone in response to mechanical stress', *Science*, Vol. 137, No. 3535, pp.1063–1064.

Becker, R., Bassett, C. and Bachmann, C. (1964) 'Bioelectric factors controlling bone structure', in Frost H. (Ed.): *Bone Biodynamics*, Little, Brown and Co., Boston, p.209.

Beer, G. (2001) *Programming the Boundary Element Method: An Introduction for Engineers*, John Wiley & Son, UK.

Beer, G., Smith, I. and Duenser, C. (2008) *The Boundary Element Method with Programming*, Springer Wien, New York.

Biot, M.A. (1956) 'General solutions of equations of elasticity and consolidation for a porous material', *J. Appl. Mech*, Vol. 78, pp.91–96.

Blokhuis, T.J., den Boer, F.C., Bramer, J.A.M., Jenner, J.M.G.Th., Bakker, F.C., Patka, P. and Haarman, H.J.Th.M. (2001) 'Biomechanical and histological aspects of fracture healing, stimulated with osteogenic protein-1', *Biomaterials*, Vol. 22, pp.725–730.

Brebbia, C.A. and Domínguez, J. (2003) *Boundary Element: An Introductory Course*, Computational Mechanics Publications, UK.

Brown, T.D., Pedersen, R., Gray, M.L. and Rubin, T. (1990) 'Toward an identification of mechanical parameters initiating periosteal remodeling: a combined experimental and analytic approach', *J. Biomech.*, Vol. 9, pp.893–905.

Caplan, A.I. and Boyan, B.D. (1994) 'Endochondral bone formation: the lineage cascade', in Hall, B.K. (Ed.): *Mechanism of Bone Development and Growth*, CRC Press, FL.

Claes, L.E. and Heigele, C.A. (1999) 'Magnitudes of local stress and strain along bony surfaces predict the course and type of fracture healing', *Journal of Biomechanics*, Vol. 32, pp.255–266.

Claes, L.E., Heigele, C.A.. Neidlinger-Wilke, C., Kaspar, D., Seidl, W., Margevicius, K.J. and Augat, P. (1998) 'Effects of mechanical factors on the fracture healing process', *Clin. Orthop.*, Vol. 355, pp.S132–S147.

Dargush, G.F. and Banerjee, P.K. (1991) 'A boundary element method for axisymmetric soil consolidation', *Int. J. Solids Structures*, Vol. 28, pp.897–915.

Dargush, G.F and Banerjee, P.K. (1992) 'Time dependent axisymmetric thermoelastic boundary element analysis', *International Journal for Numerical Methods in Engineering*, Vol. 33, pp.695–717.

Denda, M. and Wang, C.Y. (2009) '3D BEM for the general piezoelectric solids', *Comput. Methods Appl. Mech. Engrg.*, Vol. 198, pp.2950-2963.

Doblaré, M., García, J.M. and Gómez, M.J. (2004) Modeling bone tissue fracture and healing: a review', *J. Engineering Fracture Mechanics*, Vol. 71, pp.1809–1840.

Duda, G.N., Kirchner, H., Wilke, H-J. and Claes, L. (1998) 'A method to determine the 3-D stiffness of fracture fixation devices and its application to predict interfragmentary movement', *Journal of Biomechanics*, Vol. 31, pp.247–252.

El-Naggar, A.M., Abd-Alla, A.M. and Mahmoud, S.R. (2001) 'Analytical solution of electro-mechanical wave propagation in long bones', *Appl. Math. Comput.*, Vol. 119, pp.77–98.

Epari, D.R., Taylor, W.R., Heller, M.O. and Duda, G.N. (2006) 'Mechanical conditions in the initial phase of bone healing', *Clinical Biomechanics*, Vol. 21, pp. 646–655.

Fleischli, J.G. and Laughlin, T.J. (1997) 'Electrical stimulation in wound healing', *J. Foot Ankle. Surg.*, Vol. 36. No. 6, pp.457–461.

Fukada, E. and Yasuda, I. (1957) 'On the piezoelectric effect of bone', *J. Phys. Soc.*, Vol. 12, No. 10, Japan, pp.1158–1162.

Gámez, B., Ojeda, D., Divo, E., Kassab, A. and Cerrolaza, M. (2007) 'Crack analysis in cortical bone using the boundary element method', Paper presented at the *III International Congress on Computational Bioengineering*, 17–19 September, Margarita-Venezuela.

García, J.M., Kuiper, J.H., Gómez, M., Doblaré, M. and Richardson, J. (2007) 'Computational simulation of fracture healing: Influence of interfragmentary movement on the callus growth', *Journal of Biomechanics*, Vol. 40, No. 7, pp.1467–1476.

Gaul, L., Kölg, M. and Wagner, M. (2003) *Boundary Element Methods for Engineers and Scientists*, Springer-Verlag, Berlin Heidelberg, Germany, ISBN 3-540-00463-7.

Gjelsvik, A. (1973) 'Bone remodeling and piezoelectricity-II and II', *J. Biomech.*, Vol. 6, pp.69–77, 187–193.

González, Y., González, C. and Cerrolaza, M. (2008) 'Modeling bone healing by boundary element method', *Rev. Int. Métodos Numéricos para Cálculo y Diseño en Ingeniería*, Vol. 24, No. 2, pp.115–136 (in Spanish).

González, Y., Cerrolaza, M. and González, C. (2009) 'Poroelastic analysis of bone tissue differentiation by using the boundary element method', *J. Engineering Analysis with Boundary Elements*, Vol. 33, pp.731–740.

Gómez, M.J., García-Aznar, J.M., Kuiper, J.H. and Doblaré, M. (2005) 'Influence of fracture gap size on the pattern of long bone healing: a computational study', *Journal of Theoretical Biology*, Vol. 235, No. 1, pp.105–119.

Graciani, E., Mantic, V., Paris, F. and Blazquez, A. (2005) 'Weak formulation of axisymmetric frictionless contact problems with boundary elements application to interface cracks', *J. Comp. Estruc.*, Vol. 83, pp.836–855.

Hernández, C.J., Beaupré, G.S., Marcus, R. and Carter, D.R. (2001) 'A theoretical analysis of the contributions of remodeling space, mineralization, and bone balance to changes in bone mineral density during alendronat treatment', *Bone*, Vol. 29, No. 6, pp.511–516.

Isaksson, H., Wilson, W., Van Donkelaar, C.C., Huiskes, R. and Ito, K. (2006) 'Comparison of biophysical stimuli for mechano-regulation of tissue differentiation during fracture healing', *Journal of Biomechanics*, Vol. 39, pp.1507–1516.

Marino, A. and Becker, R. (1970) 'Piezoelectric effect and growth control in bone', *Nature*, Vol. 228, pp.473–474.

Martínez, G., García Aznar, J.M., Doblaré, M. and Cerrolaza, M. (2006) 'External bone remodeling through boundary elements and damage mechanics', *Mathematics and Computers in Simulation*, Vol. 73, pp.183–199.

Lacroix, D. and Prendergast, P.J. (2002) 'A mechano-regulation model of tissue differentiation during fracture healing: analysis of gap size and loading', *Journal of Biomechanics*, Vol. 35, pp.1163–1171.

Lacroix, D., Prendergast, P.J., Li, G. and Marsh, D. (2002) 'Biomechanical model to simulate tissue differentiation and bone regeneration: application to fracture healing', *Medical & Biological Engineering & Computing*, Vol. 40, p.1421.

Ojeda, D., Gámez, B., Divo, E., Kassab, A. and Cerrolaza, M. (2007) 'Cavity detection in cortical bone using the BEM/GA algorithms', Paper presented at the *III International Congress on Computational Bioengineering*, 17–19 September, Margarita-Venezuela.

Ojeda, D., Divo, E., Kassab, A. and Cerrolaza, M. (2008) 'Cavity detection in biomechanics by an inverse evolutionary point load BEM technique', *J. Inverse Problems in Science and Engineering*, Vol. 16, No. 8, pp.981–993.

Papathanasopoulou, V.A., Fotiadis, D.I., Foutsitzi, G. and Massalas, C.V. (2002) 'A poroelastic bone model for internal remodeling', *International Journal of Engineering Science*, Vol. 40, pp.511–530.

Ramtani, S. (2008) 'Electro-mechanics of bone remodelling', *International Journal of Engineering Science*, Vol. 46, pp.1173–1182.

Schmidt-Rohlfinga, B., Schneidera, U., Goosta, H. and Silnyb, J. (2002) 'Mechanically induced electrical potentials of articular cartilage', *Journal of Biomechanics*, Vol. 35, pp.475–482.

Sfantos, G.K. and Aliabadi, M.H. (2007) 'Total hip arthroplasty wear simulation using the boundary element method', *Journal of Biomechanics*, Vol. 40, pp.378–389.

Silva, C.C., Thomazinib,D., Pinheiroc, A.G., Aranhad, N., Figueire, S.D., Gesf, J.C. and Sombra, A.S. (2001) 'Collagenhydroxyapatite films: piezoelectric properties', *Materials Science and Engineering B*, Vol. 86, No. 3, pp.210–218.

Stains, J.P. and Civitelli, R. (2005) 'Cell-to-cell interactions in bone', *Biochemical and Biophysical Research*, Vol. 328, No. 3, pp.721–727.

Thoeni, K. (2005) *Effiziente Berechnung anisotroper Fundamentallösungen für die Methode der Randelemente*, Master's Thesis, Graz University of Technology, Austria (in German).

Zeman, M. and Cerrolaza, M. (Eds.) (2005) 'A coupled mechanical-biological computational approach to simulate antiresorbtive-drugs effects on osteoporosis', *Computational Modelling of Tissue Surgery*, WIT Press, UK.